FEBS Letters 583 (2009) 542–548

FEBS Letters

journal homepage: www.FEBSLetters.org

Nitric oxide accumulation is required to protect against iron-mediated oxidative stress in frataxin-deficient Arabidopsis plants

Mariana Martin [a], María José Rodríguez Colman [a], Diego F. Gómez-Casati [b], Lorenzo Lamattina [a], Eduardo Julián Zabaleta [a,*]

[a] Instituto de Investigaciones Biológicas (IIB), Facultad de Ciencias Exactas y Naturales, CONICET-Universidad Nacional de Mar del Plata, C.C. 1245 (7600) Mar del Plata, Argentina
[b] Instituto de Investigaciones Biotecnológicas-Instituto Tecnológico de Chascomús (IIB-INTECH-CONICET/UNSAM), C.C. 164 (7130) Chascomús, Argentina

ARTICLE INFO

Article history:
Received 16 December 2008
Accepted 18 December 2008
Available online 27 December 2008

Edited by Barry Halliwell

Keywords:
Frataxin
Nitric oxide
Iron
Oxidative stress
Arabidopsis thaliana

ABSTRACT

Frataxin is a mitochondrial protein that is conserved throughout evolution. In yeast and mammals, frataxin is essential for cellular iron (Fe) homeostasis and survival during oxidative stress. In plants, frataxin deficiency causes increased reactive oxygen species (ROS) production and high sensitivity to oxidative stress. In this work we show that a knock-down T-DNA frataxin-deficient mutant of *Arabidopsis thaliana* (*atfh-1*) contains increased total and organellar Fe levels. Frataxin deficiency leads also to nitric oxide (NO) accumulation in both, *atfh-1* roots and frataxin null mutant yeast. Abnormally high NO production might be part of the defence mechanism against Fe-mediated oxidative stress.

1. Introduction

Frataxin is a mitochondrial protein highly conserved in mammals, yeast, bacteria and plants. This strongly suggests that frataxin is an essential protein that could play similar roles in many organisms. In humans, mutations in the frataxin gene are responsible for the cardio-neuro degenerative disease Friedreich's ataxia [1]. Several functions for this protein have been proposed including its participation in iron homeostasis [1,2], Fe–S cluster assembly and biosynthesis [3–5], respiration and oxidative phosphorylation [6,7], regulation of respiration and control of antioxidant defences [8], iron chaperone modulating mitochondrial aconitase activity [9], among others. Additionally, recombinant frataxin have been shown to interact with the iron–sulphur (Fe–S) scaffold protein IscU and the Fe–S proteins, ferrochelatase and mitochondrial aconitase [9–13]. In many organisms, frataxin deficiency is associated with Fe accumulation in mitochondria and oxidative stress. Iron detoxification seems to be an important function of frataxin relevant in anti-oxidant defence. In that sense, frataxin deficiency increases the sensitivity of yeast cells to oxidative stress [14,15].

In plants, one Arabidopsis homologous gene (*AtFH*) has been identified [16]. This gene is able to complement null mutant yeast (*Δyfh*) strongly indicating functional similarities. Two knock-outs and one knock-down T-DNA insertional mutants have been recently analysed. The knock-out mutants (*atfh-2* and *atfh-3*) present an embryo lethal phenotype, indicating an essential role of frataxin [17,18]. The knock-down mutant (*atfh-1*) plant has reduced frataxin mRNA and protein levels. In this mutant, the activity of two Fe–S containing enzymes, mitochondrial aconitase and succinate dehydrogenase, is reduced whereas malate dehydrogenase which does not contain Fe–S moiety remains almost unaltered, indicating a role of frataxin in Fe–S cluster assembly and/or insertion [17]. Recently, it was reported that AtFH can rescue frataxin-deficient RNAi *Trypanosoma brucei* cells restoring activities of Fe–S proteins [19]. Mutant plants exhibit also increased of both, ROS formation and transcript levels of oxidative stress response genes. These results indicate that frataxin is an essential protein in plants, required for full activity of mitochondrial Fe–S proteins and plays a protective role against oxidative damage [17].

In this work, it is shown that frataxin-deficient plants, *atfh-1* show a hairy root phenotype, increased iron content and high NO levels. Accumulation of NO mediates the hairy root phenotype and is required for ferritin genes' (*FER1* and *FER4*) induction to diminish free Fe. High NO content might thus be part of the defence mechanism to counteract Fe-mediated oxidative stress. Indeed, frataxin deficiency could at least be partially compensated by an increase in NO content, which might help to enhance resistance to oxidative stress.

* Corresponding author. Fax: +54 223 475 31 50.
E-mail address: ezabalet@mdp.edu.ar (E.J. Zabaleta).

0014-5793/$34.00
doi:10.1016/j.febslet.2008.12.039

2. Materials and methods

2.1. Plant materials and growth conditions

Frataxin-deficient *Arabidopsis thaliana* mutant (T-DNA insertional mutant SALK_122008 termed *atfh-1*, [17]) seedlings were grown in a growth room on AtS agar medium as described by Estelle and Somerville [20]. Plants were grown at 25 °C with 12 h. daylight at 200 μmol m^{-2} s^{-1}.

2.2. Preparation of enriched mitochondrial fractions and iron quantification

All procedures were performed at 4 °C. Starting material for mitochondrial preparations was ~4 g of Arabidopsis roots of plants grown in hydroponia during fifty days. Root tissue was processed to obtain mitochondrial enriched fraction as described [21]. To assess the enrichment of mitochondrial preparations, a western blotting using an antibody against a known mitochondrial complex I subunit (gamma Carbonic Anhydrase 2, CA2) was used (Supplementary Fig. 1).

Enriched mitochondrial samples of roots were digested completely in 2 N HCl at 95 °C. Total and organellar iron was quantified by the ferrozine method [22] which implies an initial treatment with acid to release complexed iron, reduction and quantification with ferrozine reagent. Experiments were repeated at least three times with three samples each. Statistical significance of differences between mean values was determined using ANOVA on ranks.

2.3. Root hair analysis

Analysis of root hair patterns was performed by light microscopy in a Nikon Eclipse E200 microscope. Roots were fixed with FAA solution (ethanol:water:formaldehyde:acetic acid, 10:7:2:1, v/v) for 48 h and stained with Toluidine blue and micrographs were recorded with a Nikon Coolpix 990 digital camera attached to the microscope. Statistical significance of differences between mean values was determined using Student's *t* test.

2.4. RT-PCR analysis

Total RNA was extracted from plant material using Trizol reagent (Invitrogen). Two micrograms RNA was used to synthesize cDNA, and semiquantitative RT-PCR analyses were performed on the amplification products after 16 to 35 cycles to obtain data during the exponential phase of the PCR reaction. The following primers were used to amplify cDNAs: *FER4*fw: 5′-ATGCTTCTCAAGACTGTTTCTTCAT-3′ *FER4*rv: 5′-AGCGAGTGAGAGATGAGAGCTG-3′, *FER1*fw 5′-GAGTCGTGTTCCAGCCTTTC-3′ and *FER1*rv 5′-TCTCAGCATGCCCTCTCTCT-3′. Primers amplify a fragment that spans across one intron, allowing the detection of possible genomic DNA contamination. Each PCR experiment was performed three times with different cDNA sets from independent biological replicates. PCR products containing 1/50 SYBR Gold nucleic acid stain were analysed on agarose gels. Gels were scanned on a STORM 860 laser scanner (GE Healthcare bio-Sciences, Uppsala, Sweden). The fluorescent signal for each band was quantified using ImageQuant software after background correction included in the software.

2.5. NO and NO_2 (nitrite) measurement

NO was imaged using the permeable NO-sensitive fluorophore 4-amino-5-methylamino-2′,7′-difluorofluorescein diacetate (DAF-FM DA) and epifluorescence microscopy as described [23]. NO-dependent fluorescence was quantified by two methods: (i) densitometry analysis of the fluorescence signal of images acquired from the microscope and (ii) fluorescence quantification of root tip homogenates in a fluorometer. Both methods gave similar results. For fluorescence quantification, roots were loaded with DAF-FM DA for 1 h, washed, and approximately 50 mg of root tips (1.5 cm behind the apex) were homogenized in 0.5 ml HEPES/NaOH pH 7.5 buffer. The extracts were then centrifuged (15,000×*g*, 10 min) at 4 °C and the supernatants used for fluorescence quantification in a fluorometer (Fluoroskan Ascent, Labsystems, Helsinki, Finland) using D480-40 and D525-30 filters (Chroma Technology Corp, Rockingham, VT, USA) for excitation and emission, respectively. Roots without DAF-FM DA addition were similarly processed and the fluorescence value used as a blank. Where is indicated AtS media was added with either 1 mM L-NAME, 100 μM sodium tungstate or 100 μM KCN or without addition (control). Experiments were repeated at least six times with five roots each. Data are presented as mean fluorescence intensity. NO_2 was measured using the Griess Reagent (Promega). Five hundred milligrams from 5 day old seedlings were homogenized in PBS buffer pH 7.4 following the manufacturer's specifications. Statistical significance of differences between mean values was determined using ANOVA on ranks.

2.6. Oxidative stress

Cell death as an estimation of sensitivity to oxidative stress was monitored by staining Arabidopsis roots with Evan's blue dye (Merck, Darmstadt, Germany). Wild-type and *atfh-1* seedlings were grown in AtS agar medium for 5 days and transferred to an AtS liquid medium containing 0 or 1 mM cPTIO (2-(4-carboxyphenyl)-4,4,5,5-tetramethylimidazoline-1-oxyl-3-oxide, potassium salt) for 1 h. for sequestering NO. Afterwards, 0 or 20 mM H_2O_2 was added for 1 h. After washing, roots were incubated with Evan's blue 0.5% for 30 min, washed with distilled water and photographed under a binocular (Nikon SMZ 800) for qualitative analyses. For quantitative analyses, 1 cm of treated roots were incubated with di-methyl sulfoxide (DMSO) for 30 min with shaking at room temperature, centrifuged at 12,000×g and quantified spectrophotometrically at 565 nm (Hitachi, U-1800). Determinations were performed at least six times with 30 roots of wild-type or *atfh-1* seedlings. Statistical significance of differences between mean values was determined using ANOVA on ranks.

3. Results

3.1. Frataxin-deficient plants accumulate iron

Frataxin-deficient yeast and mammals accumulate iron in mitochondria [1,2,14,15,24]. In order to study the *AtFH* gene (At4g03240) function in plants, it was determined in total and in mitochondrial enriched fractions, the Fe content of both, *atfh-1* and wild-type root cells. As shown in Fig. 1A and B, the mutant line displays ~60% more total Fe/g of dry weight and ~20% more organellar Fe than wild-type. Similar results were obtained using flower and leaves (data not shown).

The Fe storage protein ferritin accumulates in response to increased cellular Fe levels [25]. Even though the presence of ferritin was demonstrated only for plastids [26,27], it is likely to be also present in plant mitochondria [28,29]. Arabidopsis *FERRITIN 4* gene (At2g40300 – *FER4*) encodes a protein with a predicted signal peptide being the only plant ferritin with high score for both, plastids and mitochondria, although it was not found in mitochondrial proteomes yet. Since a peptide recognized by an anti-ferritin antibody is present in Arabidopsis mitochondria [29], FER4 could be a dual

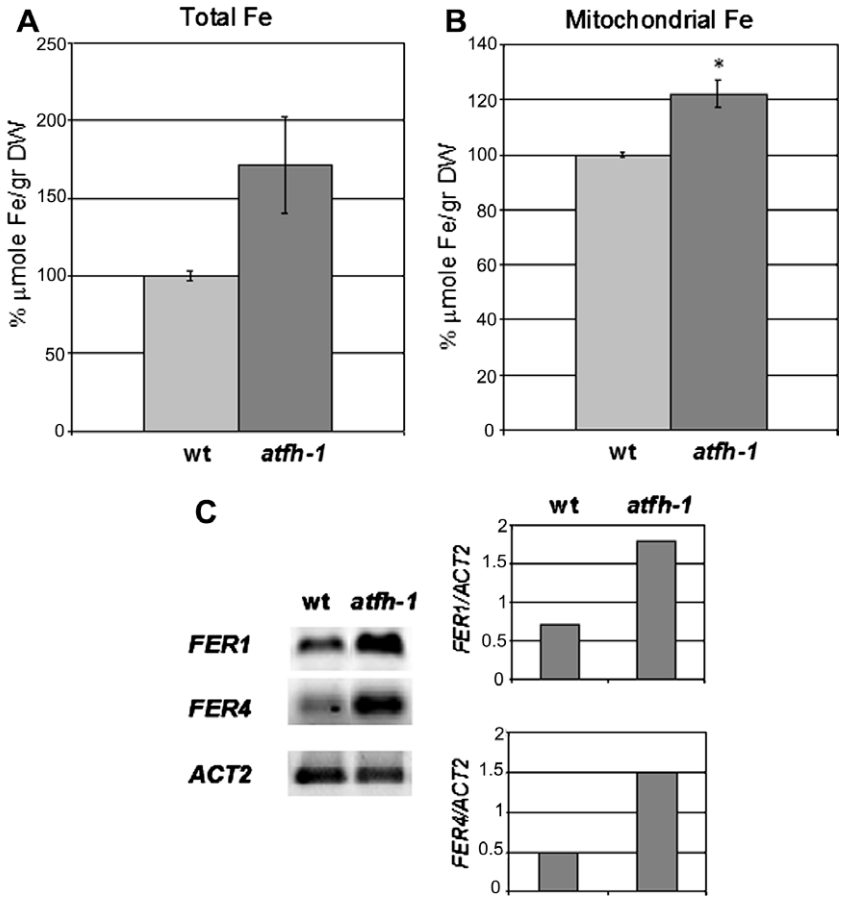

Fig. 1. Increased iron in *afth-1* root cells. Analysis of total (A) and mitochondrial (B) iron content in wt and *atfh-1* roots. Plants grown in normal conditions were used to determine mitochondrial iron content. The data (mean ± S.D.) are representative of three independent experiments. (C) *FERRITIN1 (FER1)* and *FERRITIN4* (*FER4*) expression levels are increased in *atfh-1* roots. Wild-type and *atfh-1* seedlings were grown for 15 days on AtS-agar medium. RNAs were prepared from roots and used to synthesize cDNA to perform semiquantitative RT-PCR analysis. *ACTIN 2* (*ACT2*) was used as control. *FER1*, *FER4* and *ACT2* signals were obtained during the exponential phase of the PCR reaction (left panel). Quantification of *FER1* and *4* signals in wild-type and *atfh-1* roots relative to the *ACT2* signal (right panel). Asterisks mean significant difference ($P < 0.05$).

targeting protein. Thus, induced *FER4* expression in *atfh-1* roots would reflect accumulation of iron in mitochondria and plastids suggesting *FER4* may have a protective role when iron is in excess. *FERRTIN1* (*FER1*) and *FER4* transcripts in *atfh-1* and wt roots were analysed by semiquantitative RT-PCR. As shown in Fig. 1C, *atfh-1* seedlings present higher (2.5-and 3-fold) *FER1* and *FER4* transcript levels in roots compared to the wt. These results indicate that ferritin genes indeed respond to an increased Fe level inside organelles most likely to protect against free iron. These observations further support that frataxin deficiency causes an accumulation of intracellular Fe in plants.

The main Fe uptake system in plants consists in an Fe (III) chelate reductase encoded by *FRO2* gene, the plasma membrane transporter encoded by *IRT1* gene and their regulator *FRU/FIT* [30–32]. These genes were shown to be induced by Fe deficiency conditions and repressed by Fe overload [33,34]. The *atfh-1* roots show slightly reduced steady state of *FRO2* and *IRT1* transcript levels compared to wild-type roots (data not shown) which is consistent with increased iron content in *atfh-1* roots.

Taken together, these results suggest that frataxin may be an important component to keep iron homeostasis in plants.

3.2. afth-1 roots show abnormally high nitric oxide levels

Early reports support a biological action of NO on the availability and/or delivery of metabolically active Fe within the plant [35]. Moreover, it was demonstrated that NO levels are increased in response to either iron deprivation or overload suggesting that NO is a key component of the regulatory mechanisms that control plant iron uptake and homeostasis [23,36]. Since *atfh-1* plants show increased iron levels, endogenous NO content was determined using DAF-FM DA probe in roots of *atfh-1* and wt seedlings. As shown in Fig. 2A and B, *atfh-1* roots display higher (1.5-fold) NO-dependent fluorescence than control wt roots. Fluorescence is not observed in *atfh-1* roots incubated with the NO scavenger cPTIO indicating the specificity for NO of the fluorescent signal (data not shown). To confirm fluorescent data, nitrite (NO_2^-), which is one of two primary, stable and non-volatile breakdown products of NO was measured by a diazotization reaction [37]. It was found a significant increase (1.8-fold) in nitrite content in *atfh-1* compared to that in wt plants. Incubation with cPTIO decreases 80% the nitrite content indicating the specificity of the obtained product (see Supplementary Fig. 2).

Morphological analyses indicate that *atfh-1* roots present more abundant root hair formation than wild-type roots (Fig. 2C). Root hair density was then quantified showing a ~60% increased in the mutant. Since high NO levels mediate root hair development [38], it was analysed if the high root hair density present in *atfh-1* roots relies on the observed higher NO content. *atfh-1* seedlings treated with the NO scavenger cPTIO showed a reduced root hair density (Fig. 2C). The cPTIO-dependent reduction of root hair density was dose-dependent attaining the levels observed in wt seedlings (Fig. 2C). It was reported that high production of NO is required for FER1 induction [39]. *atfh-1* roots show both *FER1* and *FER4*

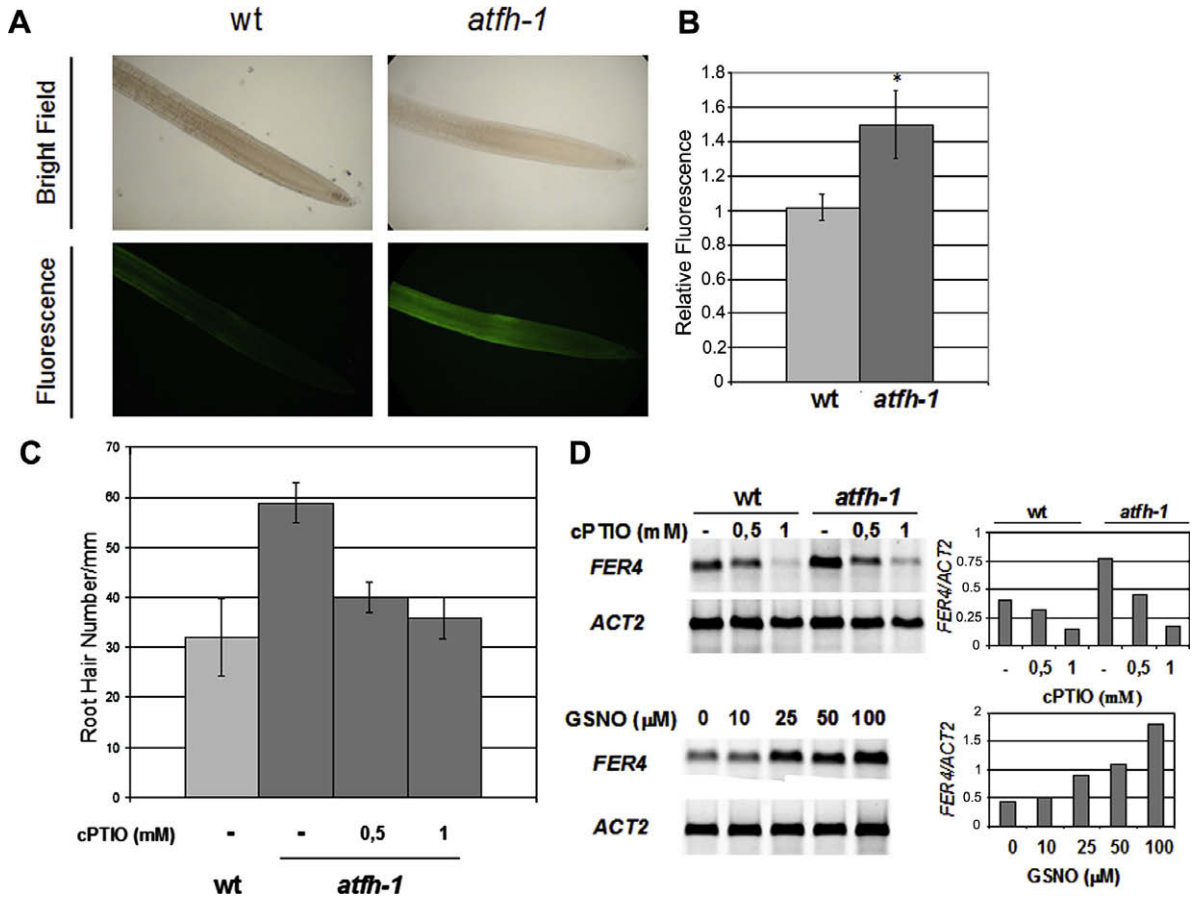

Fig. 2. High NO levels mediate the hairy root phenotype and FER4 induction. (A) NO production shown as a green fluorescence from the NO-sensitive dye DAF-FM DA in roots of wild-type and *atfh-1* seedlings. Roots of 13-day-old seedlings were incubated with DAF-FM DA for 1 h. Images from the root hair zone from primary root were acquired from the microscope. (B) Photographs were analysed with the Gel Pro Analysis 4.0 software and fluorescent molecules were extracted from root tip homogenates and was quantified in a fluorometer. Data are from six independent experiments ($n = 30 \pm$ S.D.). Asterisks mean significant difference ($P < 0.05$). (C) Ten-day-old *atfh-1* seedlings were transferred to AtS media in the presence of 0.5 and 1 mM cPTIO or without addition (control) for 3 days. Root hair density (root hairs per mm of primary root) was determined. Wild-type seedlings were used as a control. Data are representative from three independent experiments ($n = 15 \pm$ S.D.). (D) Wild-type and *atfh-1* seedlings were grown for 10 days on AtS-agar medium and transferred to AtS medium containing cPTIO or GSNO as indicated for additional 3 days. Roots were used to prepare total RNA, synthesize cDNA to perform semiquantitative RT-PCR analysis. *ACT2* was used as control. *FER4* signals were obtained during the exponential phase of the PCR reaction (left panel). Quantification of *FER4* signals in wild-type and *atfh-1* roots relative to the *ACT2* signal (right panel).

induction. It was thus analysed if *FER4* induction was also dependent of NO levels. Incubation with cPTIO reduces *FER4* levels in both wild-type and *atfh-1* roots (Fig. 2D, upper panel). Moreover, GSNO, a NO donor, induces *FER4* transcript in a dose-dependent manner (Fig. 2D, lower panel). This was not assayed in *atfh-1* roots because a higher concentration of NO could be toxic [40]. Thus, it is concluded that NO is also required for *FER4* induction. These results indicate that NO production is increased in *atfh-1* roots which mediates the hairy phenotype and induction of ferritin gene expression.

To gain insight about the main source of NO generated in *atfh-1* roots, inhibitors of NO-synthesizing pathways were used. The two most studied enzymatic sources of NO in plants are a NO synthase (NOS)-type enzyme and nitrate reductase (NR) [41]. NOS catalyzes the conversion of L-arginine to L-citruline and NO; the L-arginine analogous L-NAME has been extensively used to inhibit NOS activity in plants [42] even if a NOS homologous enzyme was not found in plants yet. NR is a molybdenum-containing enzyme that, besides its activity of nitrite generation from nitrate, catalyzes the formation of NO through nitrite reduction. Tungstate is a molybdate analog that inhibits the formation of an active NR in vivo [43] and was also shown to block NR-dependent NO generation [44]. In addition, it was demonstrated that roots are able to reduce nitrite to NO via mitochondrial electron transport [45]. KCN was then used to inhibit mitochondrial electron transport. NO production was examined with the DAF-FM DA probe in *atfh-1* and wt roots treated with L-NAME, KCN or tungstate. L-NAME and KCN substantially suppressed NO accumulation in *afth-1* roots while 1 mM tungstate did not (Fig. 3A and B). In conclusion, the increased NO production in *atfh-1* roots seems to proceed by a NOS-like activity and the electron transport chain.

Null mutant yeast lacking the frataxin gene (*Δyfh*) shows increased mitochondrial iron content, making this strain hypersensitive to oxidative stress [14]. A chimeric construct containing a mitochondrial signal peptide and the plant homolog to frataxin (*Δyfh + AtFH*) restores normal phenotype [16]. To study if the increased NO production observed in *atfh-1* plants is a general response to the frataxin deficiency, endogenous NO content was determined with the DAF-FM DA probe in wt, *Δyfh* and *Δyfh + AtFH* restored yeast cells. As was observed in *Arabidopsis* roots, frataxin deficiency produces higher NO levels (inhibited as well by L-NAME and KCN) than control wt yeast. Restored *Δyfh* cells expressing *AtFH* show normal NO content (data not shown). The observed increase in NO content is then dependent on frataxin deficiency.

3.3. High NO content protects from oxidative stress

Increased NO levels in *atfh-1* roots could protect from oxidative stress and reduce ROS-mediated cell death. To test this hypothesis,

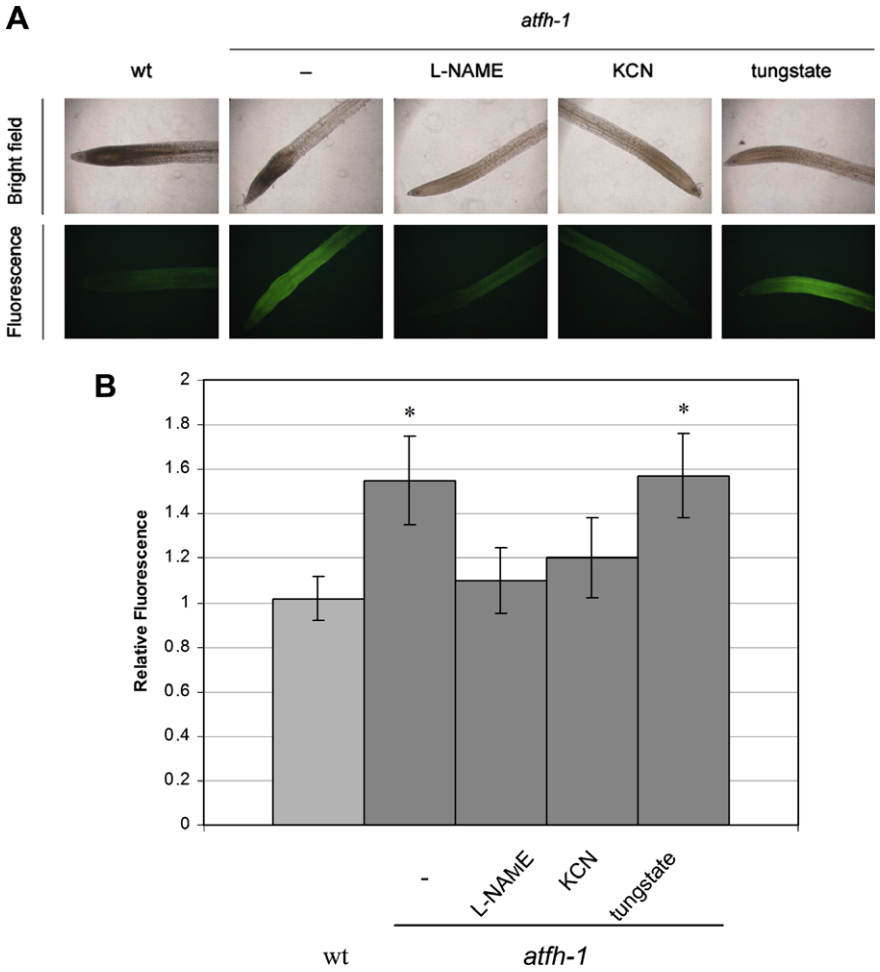

Fig. 3. Source of NO in atfh-1 seedlings. NO production in the root-hair zone of *atfh-1* seedlings in the presence of the NOS inhibitor L-NAME (*atfh-1* + L-NAME), the NR inhibitor tungstate (*atfh-1* + tungstate) or the mitochondrial electron transport inhibitor KCN (*atfh-1* + KCN). Ten-day-old seedlings were transferred to AtS media in the presence of either L-NAME, tungstate, KCN or without addition (control) for 72 h and incubated with DAF-FM DA for 1 h. Images from the young root hair zone were acquired from the microscope. (B) Photographs were analysed with the Gel Pro Analysis 4.0 software. Data are representative from three independent experiments ($n = 15$). Wild-type seedlings without addition are shown. Asterisks mean significant difference ($P < 0.05$).

seedlings were incubated with or without hydrogen peroxide in the presence of cPTIO to scavenge NO. To monitor cell viability, treated roots were stained with Evan's blue dye, which is a molecule retained only in dead cells. Quantification of this molecule retained by roots is then a way to estimate cell death and sensitivity to oxidative stress. As shown in Fig. 4A and B, *atfh-1* roots show enhanced cell death under oxidative stress than the wild-type does. Interestingly, cell death (Fig. 4) and H_2O_2 content (Supplementary Fig. 3) significantly increased when nitric oxide was sequestered by cPTIO, even without incubation with hydrogen peroxide, suggesting that elevated endogenous NO in *atfh-1* roots might protect against endogenous oxidative damage and may help to survival.

4. Discussion

In this study, it was analysed the connection between the mitochondrial protein frataxin, iron homeostasis and nitric oxide production in Arabidopsis roots and yeast. The *atfh-1* roots show 1.6-fold increased Fe content respect to wt roots. Iron content in heart mitochondria of frataxin-deficient mouse was reported to reach almost 2-fold the normal iron content at the end of time life [24]. Moreover, null mutant *Δyfh* yeast accumulates 10 times Fe in their mitochondria than wt strain does [14]. These differences in magnitude of metal accumulation when compared yeast, mammals and plants, could be related to the amplitude of the frataxin deficiency and intrinsic characteristics of the organisms. Nevertheless, the tendency to accumulate Fe into organelles is common to all organisms defective in frataxin analysed so far.

Part of the Fe increment observed in *atfh-1* roots is due to metal accumulation in mitochondria and possibly plastids as indicated by ferritin induction. Iron seems not to be abnormally accumulated in vacuoles since the expression of the well-known iron transporters NRAMP3/4 is almost unaltered in *atfh-1* roots (data not shown). In agreement with these results, mitochondrial ferritin is accumulated in human tissues affected by frataxin deficiency [46,47]. Both, *FER-1* and *FER-4* gene inductions are mediated by NO [39, and this work]. It is therefore proposed a circuit where NO production is increased by an increased Fe levels and in turns, high NO levels would induce ferritin proteins that contributes to diminish free-Fe concentration. High NO contents may also have a futile effect inducing an increment in root hairs that would contribute to Fe uptake by expanding root surface although iron uptake system is slightly down-regulated consistent with increased Fe content.

Frataxin-deficient Arabidopsis show abnormally high ROS levels and up-regulation of several known proteins involved in response to oxidative stress [17, and this work]. This is most likely due to the observed Fe accumulation. Recently, Anderson et al. [48] reported that ectopic expression of peroxide scavenging enzymes rescues frataxin deficiency in Drosophila. The *atfh-1* roots present in-

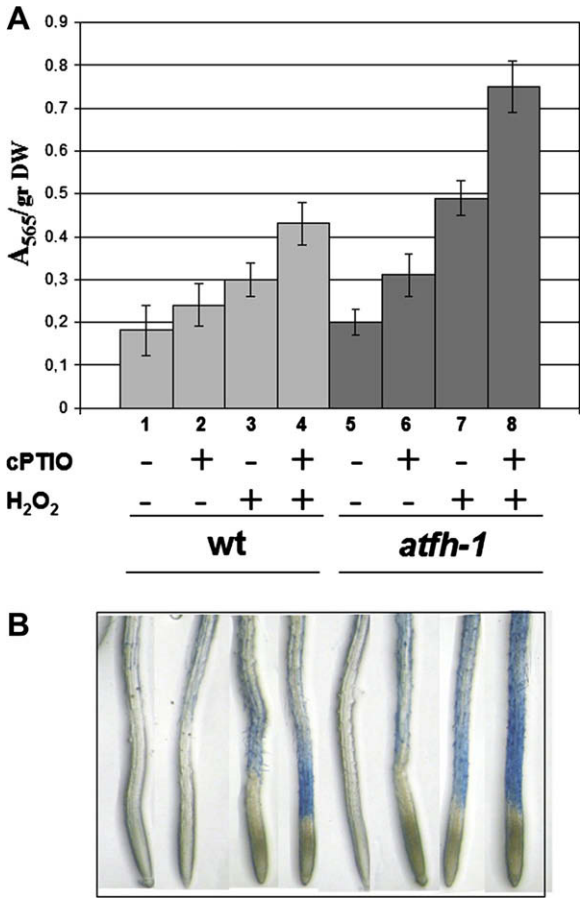

Fig. 4. High NO content in *atfh-1* roots protects from oxidative stress. Five-day-old seedling were transferred to AtS media in the presence of either 1 mM cPTIO, 20 mM H_2O_2 or both for 1 h, or without additions (control). After washings, roots were incubated with Evan's blue dye for 30 min and photographed (B). Colorant was extracted and measured at 565 nm in a spectrophotometer (A). Data are representative from six independent experiments ($n = 30 \pm$ S.D.).

creased NO levels. NO has been shown to be a potent antioxidant in plants. It was reported that this molecule could capture superoxide to reduce peroxide production [40,49]. Indeed, it was found that increased NO content in *atfh-1* roots protects from endogenous oxidative stress since scavenging NO significantly increases H_2O_2 content and cell death. This situation is more evident when incubated with exogenous hydrogen peroxide.

Taken together, these results indicate that decreased frataxin levels causes Fe accumulation. Excess of iron produces hydroxyl radicals (ROS) via the Fenton's reaction [50]. This abnormally high iron and ROS contents is paralleled by an increased NO production that protects from oxidative stress possibly by two ways: directly by scavenging peroxide and indirectly by NO-mediated induction of ferritin proteins that contributes to diminish free-Fe levels within the organelles, ROS formation and thus protecting from oxidative stress and cell death. In conclusion, higher NO production in *atfh-1* roots might be part of the response to counteract Fe-mediated oxidative stress caused by deficiency of frataxin.

Acknowledgements

We are grateful to Lic. Cristina Lombardo for technical helps in root hair analysis. This work was supported by grants from the National Agency for Science and Technology (ANPCyT, PICT 13432, 31669 and 00614), the National Research Council of Argentine (CONICET, PIP 6241) and the University of Mar del Plata, Argentina (RR 1424/05). M.M., L.L., D.G.C. and E.Z. are members of CONICET.

Appendix A. Supplementary data

Supplementary data associated with this article can be found, in the online version, at doi:10.1016/j.febslet.2008.12.039.

References

[1] Napier, I., Ponka, P. and Richardson, D.R. (2005) Iron trafficking in the mitochondrion: novel pathways revealed by disease. Blood 105, 1867–1874.
[2] Foury, F. and Talibi, D. (2001) Mitochondrial control of iron homeostasis. A genome wide analysis of gene expression in a yeast frataxin-deficient strain. J. Biol. Chem. 276, 7762–7768.
[3] Chen, O.S., Hemenway, S. and Kaplan, J. (2002) Genetic analysis of iron citrate toxicity in yeast: implications for mammalian iron homeostasis. Proc. Natl. Acad. Sci. USA 99, 16922–16927.
[4] Duby, G., Foury, F., Ramazzotti, A., Herrmann, J. and Lutz, T. (2002) A non-essential function for yeast frataxin in iron–sulfur cluster assembly. Hum. Mol. Genet. 11, 2635–2643.
[5] Lill, R. and Muhlenhoff, U. (2005) Iron–sulfur-protein biogenesis in eukaryotes. Trends Biochem. Sci. 30, 133–141.
[6] Ristow, M., Pfister, M.F., Yee, A.J., Schubert, M., Michael, L., Zhang, C.Y., Ueki, K., Michael 2nd, M.D., Lowell, B.B. and Kahn, C.R. (2000) Frataxin activates mitochondrial energy conversion and oxidative phosphorylation. Proc. Natl. Acad. Sci. USA 97, 12239–12243.
[7] Santos, R., Buisson, N., Knight, S.A., Dancis, A., Camadro, J.M. and Lesuisse, E. (2004) *Candida albicans* lacking the frataxin homologue: a relevant yeast model for studying the role of frataxin. Mol. Microbiol. 54, 507–519.
[8] Gakh, O., Park, S., Liu, G., Macomber, L., Imlay, J.A., Ferreira, G.C. and Isaya, G. (2006) Mitochondrial iron detoxification is a primary function of frataxin that limits oxidative damage and preserves cell longevity. Hum. Mol. Genet. 15, 467–479.
[9] Bulteau, A.L., O'Neill, H.A., Kennedy, M.C., Ikeda-Saito, M., Isaya, G. and Szweda, L.I. (2004) Frataxin acts as an iron chaperone protein to modulate mitochondrial aconitase activity. Science 305, 242–245.
[10] Lesuisse, E., Santos, R., Matzanke, B.F., Knight, S.A., Camadro, J.M. and Dancis, A. (2003) Iron use for haeme synthesis is under control of the yeast frataxin homologue (Yfh1). Hum. Mol. Genet. 12, 879–889.
[11] Park, S., Gakh, O., O'Neill, H.A., Mangravita, A., Nichol, H., Ferreira, G.C. and Isaya, G. (2003) Yeast frataxin sequentially chaperones and stores iron by coupling protein assembly with iron oxidation. J. Biol. Chem. 278, 31340–31351.
[12] Yoon, T. and Cowan, J.A. (2003) Iron–sulfur cluster biosynthesis. Characterization of frataxin as an iron donor for assembly of [2Fe–2S] clusters in ISU-type proteins. J. Am. Chem. Soc. 125, 6078–6084.
[13] Yoon, T. and Cowan, J.A. (2004) Frataxin-mediated iron delivery to ferrochelatase in the final step of heme biosynthesis. J. Biol. Chem. 279, 25943–25946.
[14] Babcock, M., de Silva, D., Oaks, R., Davis-Kaplan, S., Jiralerspong, S., Montermini, L., Pandolfo, M. and Kaplan, J. (1997) Regulation of mitochondrial iron accumulation by Yfh1p, a putative homolog of frataxin. Science 276, 1709–1712.
[15] Foury, F. and Cazzalini, O. (1997) Deletion of the yeast homologue of the human gene associated with Friedreich's ataxia elicits iron accumulation in mitochondria. FEBS Lett. 411, 373–377.
[16] Busi, M.V., Zabaleta, E.J., Araya, A. and Gomez-Casati, D.F. (2004) Functional and molecular characterization of the frataxin homolog from *Arabidopsis thaliana*. FEBS Lett. 576, 141–144.
[17] Busi, M.V., Maliandi, M.V., Valdez, H., Clemente, M., Zabaleta, E.J., Araya, A. and Gomez-Casati, D.F. (2006) Deficiency of Arabidopsis thaliana frataxin alters activity of mitochondrial Fe–S proteins and induces oxidative stress. Plant J. 48, 873–882.
[18] Vazzola, V., Losa, A., Soave, C. and Murgia, I. (2007) Knockout of frataxin gene causes embryo lethality in Arabidopsis. FEBS Lett. 581, 667–672.
[19] Long, S., Vávrová, Z. and Lukeš, J. (2008) The import and function of diatom and plant frataxins in the mitochondrion of *Trypanosoma brucei*. Mol. Biochem. Parasitol. 162 (1), 100–104.
[20] Estelle, M.A. and Somerville, C. (1986) Auxin-resistant mutants of *Arabidopsis thaliana* with an altered morphology. Mol. Gen. Genet. 206, 200–206.
[21] Perales, M., Eubel, H., Heinemeyer, J., Colaneri, A., Zabaleta, E. and Braun, H.-P. (2005) Disruption of a nuclear gene encoding a mitochondrial gamma carbonic anhydrase reduces complex I and supercomplex I + III2 levels and alters mitochondrial physiology in Arabidopsis. J. Mol. Biol. 350, 263–277.
[22] Tamarit, J., Irazusta, V., Moreno-Cermeño, A. and Ros, J. (2006) Colorimetric assay for the quantitation of iron in yeast words. Anal. Biochem. 351, 149–151.
[23] Graziano, M. and Lamattina, M. (2007) Nitric oxide accumulation is required for molecular and physiological responses to iron deficiency in tomato roots. Plant J. 52, 949–960.
[24] Seznec, H., Simon, D., Monassier, L., Criqui-Filipe, P., Gansmuller, A., Rustin, P., Koenig, M. and Puccio, H. (2004) Idebenone delays the onset of cardiac functional alteration without correction of Fe–S enzymes deficit in a mouse model for Friedreich ataxia. Hum. Mol. Genet. 13, 1017–1024.
[25] Petit, J.M., Briat, J.F. and Lobreaux, S. (2001) Structure and differential expression of the four members of the Arabidopsis thaliana ferritin gene family. Biochem. J. 359, 575–582.

[26] Briat, J.F., Curie, C. and Gaymard, F. (2007) Iron utilization and metabolism in plants. Curr. Opin. Plant Biol. 10, 276–282.
[27] Zybailov, B., Rutschow, H., Friso, G., Rudella, A., Emanuelsson, O., Sun, Q. and van Wijk, K.J. (2008) Sorting signals, N-terminal modifications and abundance of the chloroplast proteome. PLoS ONE 3, e1994.
[28] Zancani, M., Peresson, C., Biroccio, A., Federici, G., Urbani, A., Murgia, I., Soave, C., Micali, F., Vianello, A. and Macri, F. (2004) Evidence for the presence of ferritin in plant mitochondria. Eur. J. Biochem. 271, 3657–3664.
[29] Zancani, M., Peresson, C., Patui, S., Tubaro, F., Vianello, A. and Macrı, F. (2007) Mitochondrial ferritin distribution among plant organs and its involvement in ascorbate mediated iron uptake and release. Plant Sci. 173, 182–189.
[30] Levi, S., Corsi, B., Bosisio, M., Invernizzi, R., Volz, A., Sanford, D., Arosio, P. and Drysdale, J. (2001) A human mitochondrial ferritin encoded by an intronless gene. J. Biol. Chem. 276, 24437–24440.
[31] Varotto, C., Maiwald, D., Pesaresi, P., Jahns, P., Salamini, F. and Leister, D. (2002) The metal ion transporter IRT1 is necessary for iron homeostasis and efficient photosynthesis in *Arabidopsis thaliana*. Plant J. 31, 589–599.
[32] Henriques, R., Jasik, J., Klein, M., Martinoia, E., Feller, U., Schell, J., Pais, M.S. and Koncz, C. (2002) Knock-out of Arabidopsis metal transporter gene IRT1 results in iron deficiency accompanied by cell differentiation defects. Plant Mol. Biol. 50, 587–597.
[33] Hirsch, J., Marin, E., Floriani, M., Chiarenza, S., Richaud, P., Nussaume, L. and Thibaud, M.C. (2006) Phosphate deficiency promotes modification of iron distribution in Arabidopsis plants. Biochimie 88, 1767–1771.
[34] Duy, D., Wannee, G., Meda, A., von Wirén, N., Soll, J. and Philippar, K. (2007) PIC1, an ancient permease in Arabidopsis chloroplasts, mediates iron transport. Plant Cell 19, 986–1006.
[35] Graziano, M., Beligni, M.V. and Lamattina, L. (2002) Nitric oxide improves internal iron availability in plants. Plant Physiol. 130, 1852–1859.
[36] Arnaud, N., Murgia, I., Boucherez, J., Briat, J.F., Cellier, F. and Gaymard, F. (2006) An iron-induced nitric oxide burst precedes ubiquitin-dependent protein degradation for Arabidopsis AtFer1 ferritin gene expression. J. Biol. Chem. 281, 23579–23588.
[37] Kim, H., Shim, J., Han, P.L. and Choi, E.J. (1997) Nitric oxide modulates the c-Jun N-terminal kinase/stress-activated protein kinase activity through activating c-Jun N-terminal kinase kinase. Biochemistry 36, 13677–13681.
[38] Lombardo, M.C., Graciano, M., Polacco, J.C. and Lamattina, L. (2006) Nitric oxide functions as a positive regulator of root hair development. Plant Signal. Behav. 1, 28–33.
[39] Murgia, I., Delledonne, M. and Soave, C. (2002) Nitric oxide mediates iron-induced ferritin accumulation in Arabidopsis. Plant J. 30, 521–528.
[40] Beligni, M.V. and Lamattina, L. (1999) Nitric oxide protects against cellular damage produced by methylviologen herbicides in potato plants. Nitric Oxide 3, 199–208.
[41] del Rio, L.A., Corpas, F.J. and Barroso, J.B. (2004) Nitric oxide and nitric oxide synthase activity in plants. Phytochemistry 65, 783–792.
[42] Mackerness, A.H., John, C.F., Jordan, B.A. and Thomas, B. (2001) Early signaling components in ultraviolet-B responses: distinct roles for different reactive oxygen species and nitric oxide. FEBS Lett. 489, 237–242.
[43] Deng, M., Moureaux, T. and Caboche, M. (1989) Tungstate, a molybdate analog inactivating nitrate reductase, deregulates the expression of the nitrate reductase structural gene. Plant Physiol. 91, 304–309.
[44] Bright, J., Desikan, R., Hancock, J.T., Weir, I.S. and Neill, S.J. (2006) ABA-induced NO generation and stomatal closure in Arabidopsis are dependent on H_2O_2 synthesis. Plant J. 45, 113–122.
[45] Gupta, K.J., Stoimenova, M. and Kaiser, W.M. (2005) In higher plants, only root mitochondria, but not leaf mitochondria reduce nitrite to NO, in vitro and in situ. J. Exp. Bot. 56, 2601–2609.
[46] Michael, S., Petrocine, S.V., Qian, J., Lamarche, J.B., Knutson, M.D., Garrick, M.D. and Koeppen, A.H. (2006) Iron and iron-responsive proteins in the cardiomyopathy of Friedreich's ataxia. Cerebellum 5, 257–267.
[47] Vert, G., Grotz, N., Dedaldechamp, F., Gaymard, F., Guerinot, M.L., Briat, J.F. and Curie, C. (2002) IRT1, an Arabidopsis transporter essential for iron uptake from the soil and for plant growth. Plant Cell 14, 1223–1233.
[48] Anderson, P.R., Kirby, K., Orr, W.C., Hilliker, A.J. and Phillips, J.P. (2008) Hydrogen peroxide scavenging rescues frataxin deficiency in a Drosophila model of Friedreich's ataxia. Proc. Natl. Acad. Sci. USA 105, 611–616.
[49] Beligni, M.V., Fath, A., Bethke, P.C., Lamattina, L. and Jones, R.L. (2002) Nitric oxide acts as an antioxidant and delays programmed cell death in barley aleurone layers. Plant Physiol. 129, 1642–1650.
[50] Halliwell, B. and Gutteridge, J.M. (1992) Biologically relevant metal ion-dependent hydroxyl radical generation. An update. FEBS Lett. 307, 108–112.